Vol. 18(1), pp. 38-52, January-March, 2023
DOI: 10.5897/IJPS2022.5003
Article Number: D2AA65170400
ISSN: 1992-1950

http://www.academicjournals.org/IJPS

ACADEMIC JOURNALS
expand your knowledge

International Journal of Physical Sciences

Full Length Research Paper

A mathematical model development to investigate the impact of key parameters on the generated voltage hysteresis of silicon anode based lithium half cells

Al-Mustasin Abir Hossain

Department of Mechanical Engineering, School of Engineering and Computer Science (ENCS), Washington State University, WA, United States.

Received 29 July, 2022; Accepted 13 December, 2022

Lithium-ion batteries are widely used in various energy storage systems. In this article, a physics-based mathematical model of silicon micro-particle (SiMP) anode is developed to identify the principal reasons of voltage hysteresis occurrence during lithiation and delithiation battery cycling of silicon (Si) anode-based lithium half cells. Firstly, lithium diffusion, reaction kinetics, thermodynamics and mechanical stress and strain are selected, and relevant mathematical equations are developed. To examine the impact of hydrostatic stresses on electrochemical reactions in battery electrodes, a modified version of Butler-Volmer (BV) kinetics equation including hydrostatic stress induced voltage term is implemented. For model development, essential parameters are identified and sensitivity analysis is conducted to figure out the best fitted parametric values. Finally, a physics-based mathematical model is developed to investigate the impact of key parameters on generated voltage hysteresis of the SiMP half cells. Using this mathematical model, voltage curves are generated and fitted with the experimental results. In addition, the model is used to identify performance limitations. By examining the influence of the key parameters on the voltage curves during battery cycling, the model exhibits the principal causes of voltage differences during lithiation and delithiation. The detail of this article will provide more crucial information.

Keywords: Model, parameters, butler-volmer, hydrostatic, stress, voltage, limitations.

INTRODUCTION

Lithium-Ion batteries (LIBs) are viewed as the most useful energy storage medium for different electronic devices and heavy electric vehicles (Zhang, 2010; Jin et al., 2017; Tarascon and Armand, 2001; Boukamp et al., 1981). It has been recommended by the researchers that the durability of the LIBs can be ameliorated highly if the graphite anode in LIBs can be replaced with silicon (Si) made anode. It has been reported that silicon's energy density (3579 mAh/g) is almost ten times higher than graphite's energy density (372 mAh/g) (Tarascon and Armand, 2001; Boukamp et al., 1981; Ashuri et al., 2016; Liang et al., 2014).

E-mail: al-mustasin.hossain@wsu.edu.

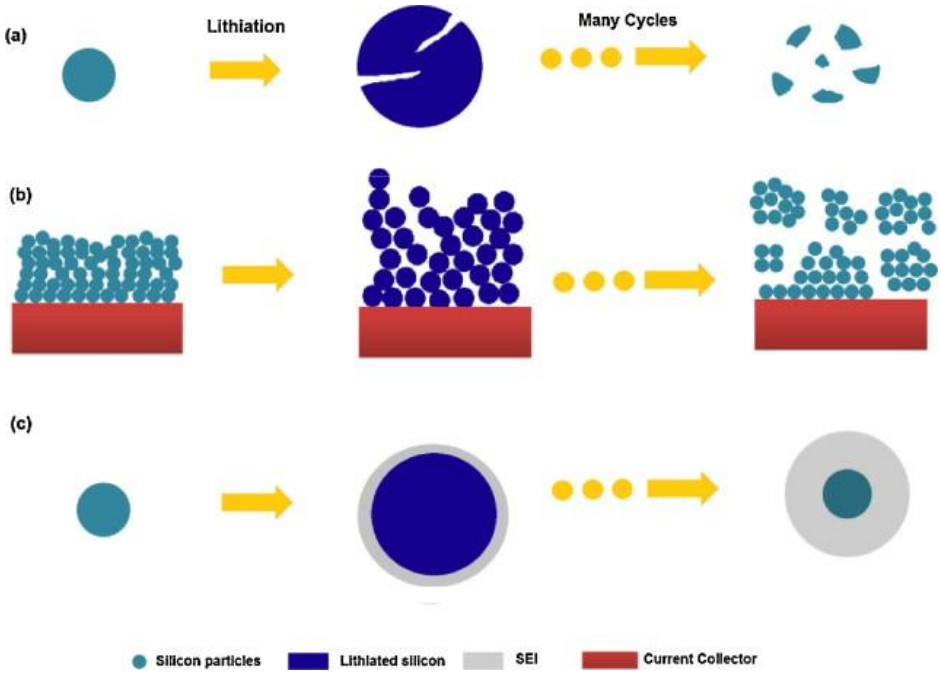

Figure 1. Si electrode failure mechanisms (a) material pulverization; (b) Morphology and volume change of the entire Si electrode (c) Continuous SEI growth layer (Wu and Cui, 2012; Di Leo et al., 2015; Verbrugge and Cheng, 2019; Sethuraman et al., 2010; Bower et al., 2011). Source: Author 2022

However, researchers discovered some problems in silicon. The main problem is that it experiences a large volume expansion (~300%) during lithiation and contraction during delithiation (Ashuri et al., 2016; Liang et al., 2014; Verbrugge et al., 2015). In the past, researchers testified that stress generation coupled with these large volume changes in Si particle is the major reason of cracking and pulverization of silicon (Si) electrodes that leads to loss of electrical conductivity and capacity fade during battery cycling (Wu and Cui, 2012; Di Leo et al., 2015; Verbrugge and Cheng, 2019; Sethuraman et al., 2010; Bower et al., 2011) as shown in Figure 1. Additionally, a huge voltage gap known as voltage hysteresis is witnessed during lithiation-delithiation cycling (Wang et al., 2017). This hysteresis is very damaging for silicon anode-based lithium-ion batteries (Baker et al., 2017). To optimize the Si-anode-battery design, a simple physics-based mathematical model that can precisely identify this reason behind this hysteresis emergence in Si is needed. Earlier, model developers and researchers worked with silicon anode based mathematical model (Jin et al., 2019; Song et al., 2016; Lu et al., 2016). But none of them validated their mathematical modeling with any experimental data. In addition to that, no one has taken volume expansion phenomena of silicon spherical particle into their account while developing their mathematical model. Li et al. (2014) reported that charging and discharging rates of lithium-ion battery electrodes should be evaluated separately due to the asymmetric effects in the chemical diffusion co-efficients during lithiation and delithiation.

They also noticed that the value of diffusivity in delithiation cycle is always higher than lithiation cycle as shown in Figure 2. The reason behind the phenomenon is that Si goes through compressive stress upon lithiation and tensile stress under delithiation and the stress fluctuation is approximately 2.0 GPa which is quite high. Nobody considered this asymmetric diffusivity phenomenon in their mathematical model development. In the current work, a physics-based mathematical half-cell model is developed which can forecast the reason behind this voltage hysteresis generation. The model development was started with one dimensional single spherical particle model. Because of having volume inconsistency in silicon, state of charge (SOC) dependent radius equation is used in this work. Then unequal diffusivity is used as Li et al. (2014) reported diffusivity cannot remain constant throughout battery cycling. In addition to that, asymmetric exchange current density is included of which nobody has ever reported. To the best of the researcher's knowledge, the researchers are the first in this field to add all these features in battery modeling. A modified version of Butler Volmer (BV) equation including stress induced voltage term likewise Jin et al. (2019) is used here. Earlier, Verbrugge and Cheng (2018) at their work experimented stress evaluation during lithiation and delithiation cycling. They developed an analytical solution to measure the influence

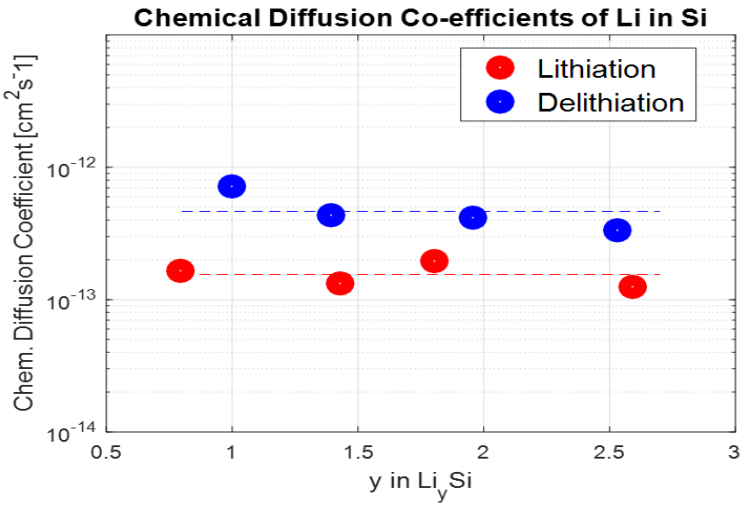

Figure 2. Chemical diffusion co-efficients of Li in Si at different SOC values measured by PITT (Li et al., 2014).
Source: Author 2022

of surface mechanics on diffusion induced hydrostatic stresses within spherical nanoparticles. The analytical solution developed by Cheng and Verbrugge (2018) is applied here to calculate stress induced voltage.

In this work, literature surveys were performed to identify the crucial parameters which are highly essential for battery model development. Next, the best parametric ranges were found, and sensitivity analysis was accomplished. After that, the best fitted value for the parameters for the model development were discovered. Then, voltage vs. specific capacity curves were produced with our own developed mathematical model. Wang et al. (2013) demonstrated self-healing chemistry of silicon active materials and conducted lithiation-delithiation cycling experiments at different C-rates. Experimental data generated by Wang et al. (2013) was used to validate our own built mathematical model. Next, we figured out the impact of the key parameters on voltage hysteresis. By including hydrostatic stress induced voltage term in the Butler-Volmer (BV) equation voltage differences were successfully captured. Finally, the main reason behind voltage hysteresis occurrence in the lithiation-delithiation cycling is identified. We figured out by controlling diffusivity and exchange current density values, voltage curves' shape can be changed. Further study will provide elaborate more explanation.

EXPERIMENT

Battery cycling test

This test was conducted by Wang et al. (2013) in their study. Their experimental data was used here to validate the results generated by our model. Self-healing chemistry of silicon active materials and lithiation-delithiation cycling experiments at different C-Rates were demonstrated by Wang et al. (2013).

They manufactured self-healing silicon electrodes by sealing SiMP's inside an SHP/CB composite layer. Coin cells with metallic lithium counter electrodes were employed to evaluate the electrochemical performance of the electrodes. On deep galvano-static cycling between 0.01 (V) and 1 (V), the lithiation capacity reached 2,617 mAh/g for the first cycle at a current density of 0.4 A/g which is about six times higher than the theoretical capacity of graphite shown in Figure 3a and b. The electrode showed good cycling stability.

Side reaction correction

During battery cycling test, each time capacity offset was noticed between beginning and closing point of the cycle as shown in Figure 4a and b. This capacity gap was generated because of side-reaction formation. Some by-products were produced when TAFEL chemical kinetics appeared at the anode-electrolyte interphase. As reported by Sethuraman et al. the appearance of TAFEL chemical kinetics can partially lead to voltage hysteresis in lithium-Ion batteries (LIBs) (Sethuraman et al., 2012; Hossain et al., 2020a; Pharr et al., 2013). The authors pointed out that the stress can also contribute to the open circuit potential (OCP) behavior to open circuit potential. Therefore, correction of side reaction is essential for battery development. It was reduced by applying side-reaction (SR) correction formula on the exchange current density (Sethuraman et al., 2012; Hossain et al., 2020; Pharr et al., 2013). Sethuraman implemented TAFEL regime formula for side-reaction correction in their work (Sethuraman et al., 2012; Hossain et al., 2020b; Pharr et al., 2013). Here same formula (Equation1) was applied for the SR correction on the exchange current density.

$$i_{0,SR} = i_0 \exp\left(\frac{\alpha_{SR} F}{R_g T}\,(V - U_{SR})\right) \quad (1)$$

The transfer coefficient for the side reaction, α_{SR}, was selected as 0.5 (Sethuraman et al., 2012; Hossain et al., 2020b; Pharr et al., 2013). While Tafel kinetics did not give a specific equilibrium

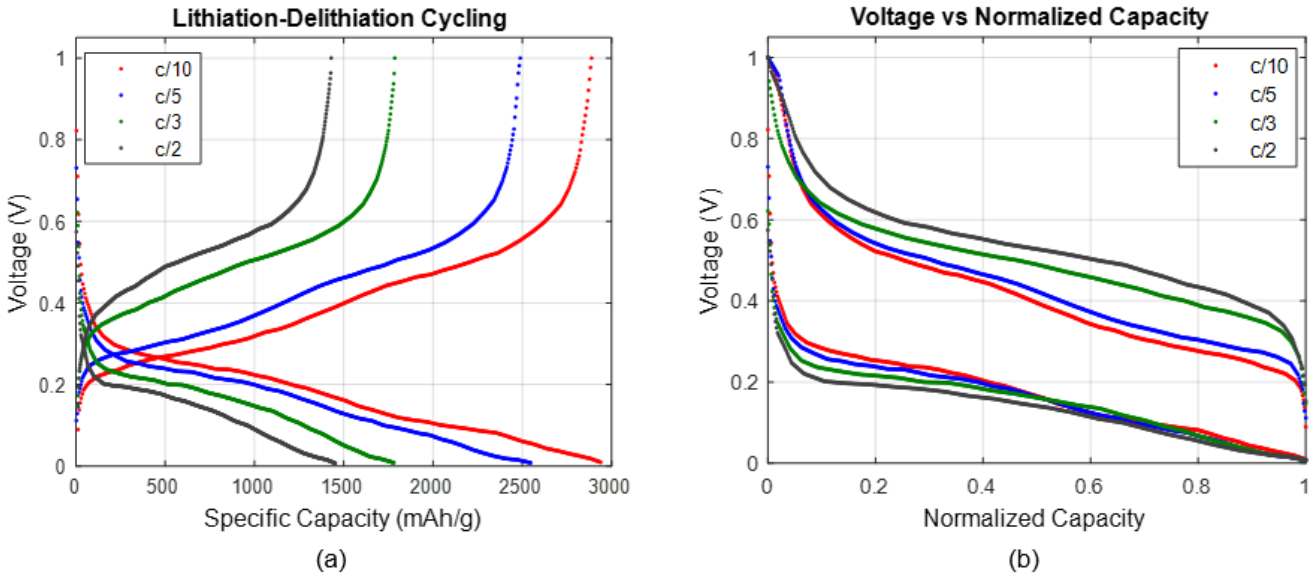

Figure 3. (a) Lithiation-delithiation cycling experiment conducted by Wang et al. (2013) at four different C-rates: C/10 (Red dots); C/5 (Blue dots); C/3 (Green dots); C/2 (Black dots); (b) Voltage vs Normalized Capacity Curve for all four different C-rates. These data are used in the validation of Mathematical Model.
Source: Author 2022

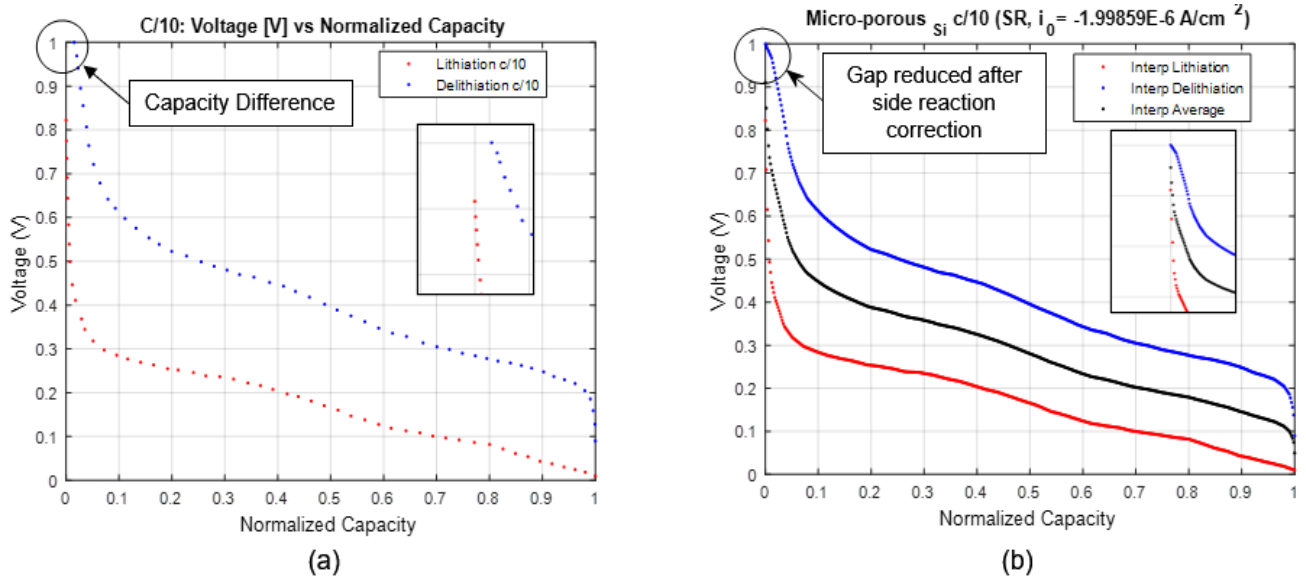

Figure 4. Lithiation-Delithiation cycling experiment of C/10; Voltage curve generated (a) Before side-reaction correction; (b) After side-reaction correction; Red dotted lines denote lithiation cycle, whereas blue dotted line shows delithiation and black dotted line display interp curve.
Source: Author 2022

potential (i_0 and U are related), we adopted a value of $U_{SR} = 0.8$ vs. Li/Li^+ to estimate $i_{0,SR}$ (Sethuraman et al., 2012; Hossain et al., 2020b; Pharr et al., 2013). This side-reaction current, $i_{0,SR}$ was then calculated through the cycle considering an i_0 such that the marching was excluded from the cycling data. The voltages we got from the experiment were implemented in this study.

Side-reaction correction technique of the battery cycling test of SiMP at C/10 C-rate was demonstrated. In Figure 4a, from the voltage vs. normalized capacity graph, capacity difference at the end of the cycling before the side reaction correction is seen. Whereas in Figure 4b, voltage vs. normalized capacity graph depicts the cycling scenario after side-reaction correction. For C/10, $i_{0,SR}$ value was calculated to be -1.99859×10^{-6} A/cm^2. The black dots in the Figure 4b are defined as the average of lithiation-

delithiation plots which was used as open circuit voltage curve in our simulation model as well. In this way, side-reaction was corrected for different C-rates such as C/5, C/3 and C/2. As various scientist (Sethuraman et al., 2012; Hossain et al., 2020b; Pharr et al., 2013) reported silicon anode has the tendency to exhibit OCP. Therefore, with side reaction correction, OCP can be minimize a bit. Pan et al. (2014) mentioned that much lower C-rates exhibits more OCP than the ones with higher C-rates. Therefore, in this work, four moderately ranged C-rates have been chosen to generate lithiation-delithiation curve.

Mathematical model development

Our main aim in the research work is to mathematically investigate the reason behind this voltage hysteresis phenomenon by parametric study. Therefore, a physics based mathematical model was developed to scrutinize the cause of voltage hysteresis occurrence. We wanted to make our model as simple as possible. So, we started development of the model considering one dimensional single particle half-cell model. The key feature in our model includes state of charge (SOC) dependent radius equation, usage of asymmetric diffusivity and asymmetric exchange current density.

Mass balance equation

Since our model is a single particle one-dimensional half-cell model, the model developed in this study assumed the silicon particle to be a single phase, rather than a two-phase system. A porous electrode model that reflects this schematic was developed to estimate the reaction distribution across the electrode. The governing equations and boundary conditions (Table 1) for this model is discussed in the literature. These equations are composed of mass balance in the solid phases and the modified Butler-Volmer (BV) equation including hydrostatic stress. These equations are used to describe the electrochemical reaction at the interface. The hydrostatic stress in the surface layer due to surface effects is composed of two parts. One depended on the average concentration c_{av} which means that the diffusion induced deformation. The other one is concentration, c_s dependent. To estimate diffusion coefficients in the particle using data, Fick's law (Equation 2) was numerically solved in spherical coordinates.

$$\frac{\partial \mathrm{c_s}}{\partial \mathrm{t}} = \mathrm{D_s}\frac{\partial^2 \mathrm{c_s}}{\partial \mathrm{r}^2} + 2\frac{\mathrm{D_s}}{\mathrm{r}}\frac{\partial \mathrm{c_s}}{\partial \mathrm{r}} \quad (2)$$

The boundary and initial conditions are set as shown in Figure 5.

$$D_s\frac{\partial c_s}{\partial r} = -\frac{i_{app}}{a_V LF}\ ;\ \text{for}\ r = R \quad (3)$$

$$D_s\frac{\partial c_s}{\partial r} = 0\ ;\ \text{for}\ r = 0 \quad (4)$$

$$c_s = c_0\ ;\ \text{for}\ t = 0 \quad (5)$$

Where R is defined as the particle radius (m), c_s is denoted as the lithium concentration (mol/m^3), c_0 is the initial lithium concentration (mol/m^3), D_s is the diffusion coefficient (m^2/s), i_{app} is the current density (A/m^2), a_V is the surface-to-volume ratio (1/m), L is cell thickness (m), and F is the Faraday's constant (C/mol). In estimating the diffusion coefficients, both particle volume changes and stress effects were ignored.

Pharr et al. (2013) studied surface cracking at the electrode. Surface cracking is directly related with surface-to-volume ratio. Surface-to-volume ratio could be calculated as follows:

$$a_V = \frac{N*4\pi R^2}{\frac{1}{\epsilon}N*\frac{4}{3}\pi R^3} = \frac{3\epsilon}{R} \quad (6)$$

Where, ϵ is volume ratio of silicon, N is the number of particles, here $N = 1$. Surface-to-volume ratio is an important parameter related with exchange current density. R is the particle radius as a function of state of charge (SOC) (m).

Modified Butler-Volmer equation

In the model, hydrostatic stress induced voltage term was included in Butler-Volmer (BV) equation. The electrode particle goes through the volumetric strain during the lithiation-delithiation battery cycling of lithium-ions as shown and results in stress generation inside the particle. This stress generation due to lithiation-delithiation in the spherical electrode particle was calculated by the hydrostatic stress as reported by Cheng (2018). Therefore, the modified Butler-Volmer (BV) equation can be expressed as:

$$j_n = \frac{i_0}{F}\left\{\exp\left[\frac{F(V-U)-\sigma_h\Omega}{2R_gT}\right] - \exp\left[-\frac{F(V-U)-\sigma_h\Omega}{2R_gT}\right]\right\} \quad (7)$$

j_n is net flux (mol/m^2/s). It can be defined as:

$$j_n = \frac{i_{app}}{a_V LF} \quad (8)$$

So, Equation (7) can be expressed as follows:

$$\frac{i_{app}}{a_V LF} = \frac{i_0}{F}\left\{\exp\left[(1-\alpha)\frac{F(V-U)-\sigma_h\Omega}{R_gT}\right] - \exp\left[-\alpha\frac{F(V-U)-\sigma_h\Omega}{R_gT}\right]\right\} \quad (9)$$

Where, σ_h is hydrostatic stress at the surface layer of electrode (N/m^2), Ω is the partial molar volume (mol/m^3), α is the symmetric coefficient, i_0 is the exchange current density (A/m^2), R_g is the universal gas constant (J/kg/K), T is the temperature (K). If we use $\alpha = 0.5$, Equation (9) can be written as (full derivation is given in the Appendix).

$$V = U + \frac{\sigma_h\Omega}{F} + \frac{2R_gT}{F}\sinh^{-1}\left(\frac{i_{app}}{2i_0a_V LF}\right) \quad (10)$$

Cheng and Verbrugge (2018) developed analytical model for hydrostatic stress calculation. Hydrostatic stress equation is expressed as:

$$\sigma_h(r_0) = \frac{2E\Omega}{9(1-\nu)}[S_1c_{av}(r_0) - c(r_0)] + S_2 \quad (11)$$

Here, S_1 and S_2 are the constants. These two can be written as:

$$S_1 = \frac{1-\frac{K^S(1+\nu)}{R_g\ E}}{1+\frac{2K^S1-2\nu}{R_g\ E}} \quad (12)$$

$$S_2 = -\frac{\frac{2\tau^0}{R_g}}{1+\frac{2K^S1-2\nu}{R_g\ E}} \quad (13)$$

Where, K^S is the surface modulus (N/m), τ^0 is the deformation-independent surface tension (J/m^2), E is denoted as Young's modulus (GPa), ν is Poisson's ratio.

Average surface concentration, c_{av} (mol/m^3) as a function of time is calculated developing following equation:

$$c_{av}(t) = c_0 + \frac{\int_0^t\frac{i_{app}(t)}{a_V FL}dt}{\epsilon a_V} = c_0 + \int_0^t\frac{i_{app}(t)}{\epsilon FL}dt \quad (14)$$

Table 1. Governing equations and boundary conditions for porous electrode (half-cell) model.

Governing equation	Boundary condition
Mass balance in solid phase (spherical coordinate) (c_s: lithium concentration)	
$\frac{\partial c_s}{\partial t} = D_s \frac{\partial^2 c_s}{\partial r^2} + 2\frac{D_s}{r}\frac{\partial c_s}{\partial r}$	$D_s \frac{\partial c_s}{\partial r}\|_{r=R} = -\frac{i_{app}}{a_V LF}$; $D_s \frac{\partial c_s}{\partial r}\|_{r=0} = 0$
Average concentration profile in solid phase	
$\epsilon FL \frac{dc_{av}(t)}{dt} = i_{app}(t)$	
Modified Butler-Volmer voltage equation	
$V = U + \frac{\sigma_h \Omega}{F} + \frac{2R_g T}{F} \sinh^{-1}\left(\frac{i_{app}}{2i_0 a_V LF}\right)$	

Source: Author2022

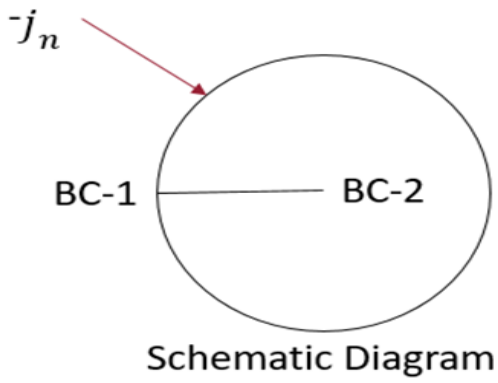

Figure 5. Schematic diagram of a spherical particle (24,28)
Source: Author2022

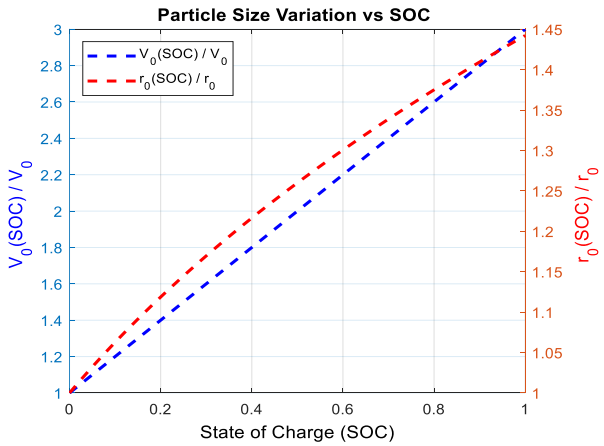

Figure 6. Working principle of particle radius as a function of SOC
Source: Author 2022

Here, c_0 is denoted as the initial molar concentration (mol/m^3) and the other parameters are the same as before. This parameter is used in hydrostatic stress calculation.

Particle radius as a function of SOC

During lithiation cycling, silicon particle in the anode experiences (~300%) volume expansion. In this regard, spherical particle's radius will also expand during lithiation. We wanted to make our model more realistic. Therefore, an important feature is added in our model development. A particle radius equation as a function of state of charge (SOC) is developed here. The equation is expressed as follows (full derivation is given in the Appendix):

$$R = r_0[1 + (2SOC)]^{\frac{1}{3}} \quad (15)$$

Here, r_0 is initial particle radius (m). State of charge (SOC) is defined as follows:

$$SOC = \frac{Avergae\ Concentration}{Maximum\ Concentration} = \frac{c_{avg}}{c_{\max}} \quad (16)$$

Since we considered 300% volume increment during lithiation, spherical particle radius cannot remain constant throughout the cycling. Therefore, particle radius will also change during lithiation-delithiation cycling experiment.

At unlithiated condition, when $SOC = 0$ the volume is constant and defined as 1. As SOC progresses, volume keeps increasing, and at fully lithiated condition when $SOC = 1$, particle experiences ~300% volume expansion means volume of the particle enlarges 3 times the initial volume.

Therefore, at fully lithiated condition, the ratio of $\frac{v_0(SOC)}{v_0}$ becomes 3. $r_0(SOC)$ can be denoted as *R*.
Similarly, $\frac{R}{r_0}$ is 1 at unlithiated condition. When *SOC* progresses and becomes 1, the particle radius ratio becomes 1.45 as shown in the Figure 6.

Asymmetric solid diffusivity and exchange current density

Another new feature added in our model is the usage of asymmetric solid diffusivity. In the past, previous researchers used constant value for solid diffusivity throughout the model. Li et al. (2014) reported lithiation and delithiation rates of lithium-ion-battery electrodes should be evaluated separately due to the asymmetric effect in the chemical diffusion coefficients during lithiation and delithiation cycling. Therefore in our work, instead of using constant values thought, two different values for solid diffusivity were used, one for lithiation cycle and another one for delithiation cycle. Likewise, asymmetric solid diffusivity, for the case of exchange

current density, two different exchange current density values was used. One for lithiation and another one for delithiation. In our case, we used unequal values as provided new insight into determining the rate-limiting component in lithium-ion batteries and identifying candidate electrodes for high-power applications. According to our knowledge, we are the first one in this field to include these unique features in modelling development.

Solution procedure

All the mathematical model equations were solved by a finite-element package COMSOL Multiphysics 5.6. Model parameters such as electrode design, thermodynamics, transport, kinetics, and mechanical properties are listed in Table 1. The experiments were conducted at Standard condition such as 25°C (room temperature) by Wang et al. (2013). Since we used their experimental data to validate our work, we also used similar four different C-rates such as C/10, C/5, C/3 and C/2 to validate our mathematical model. The validity of the parameter choice was checked by comparing the physics model to experiments, as shown in Table 2.

RESULTS AND DISCUSSION

In analyzing electrodes at high C-rates, relatively thin-layer electrodes are regarded as an ideal design because the transport limitation in the electrolyte phase is ignored. We considered ideal electrode using the porous electrode model. In addition, as Pan (2014) mentioned that low C-rates have in Si anode LIBs have the tendency to generate OCP, which is detrimental to battery. Therefore, to avoid complexity in the model development, we chose average of lithiation and delithiation voltage values for all our C/10, C/5, C/3 and C/2 C-rates as open-circuit potential values. OCP values helped the model generated curve to follow a plot trend similar to experimental curves. Before developing our own mathematical model, we conducted literature surveys (Hossain and Kim, 2020b; Tanim et al., 2015; Sikha et al., 2014; Christensen and Newman, 2006; Safari and Delacourt, 2011; Jagannathan and Chandran, 2014; Chandrasekaran et al., 2010; Zhang et al., 2007; Hossain et al., 2020; Masud et al., 2021; Hossain et al., 2022a; Hossain et al., 2022b; Ojeda et al., 2022) figured out the parameters required to develop a battery model. Next, the best possible ranges were discovered for those parametric values. Next, key parameters which have impact on voltage hysteresis were found, and sensitivity analyses were conducted with all four different C-rates.

Impact of sensitivity analysis

From our literature surveying we noticed solid diffusivity, exchange current density, partial molar volume, Young's modulus and Poisson's ratio can be identified as the main parameters which have influence on voltage hysteresis. Using our mathematical model, sensitivity analysis with these key parameters was performed by generating voltage curves at C-rates of C/10, C/5, C/3 and C/2. The proceedings were started with five different values of solid diffusivity, D_l in lithiation cycle. The limits of solid diffusivity in both lithiation and delithiation cycle were selected from 1.0×10^{-15} m^2/s to 1.0×10^{-11} m^2/s. These ranges were selected by reviewing several papers. Once the best fitted results were found, we moved to solid diffusivity, D_d in delithiation cycle and executed the identical procedure. Next, we focused on exchange current density in lithiation cycle, $i_{0,l}$ and then concentrated on delithiation cycle, $i_{0,d}$. For the exchange current density, parametric ranges were chosen between 0.0001 and 10.0 A/m^2. For other crucial parameters such as partial molar volume, we used constant values during the lithiation-delithiation cycling and the limit was selected from 1.0×10^{-7} to 1.0×10^{-5} mol/m^3 and for other two parameters, Young's modulus, E and Poisson's ratio, ν the parametric ranges were chosen as from 50 to 250 GPa and from 0.10 to 0.45 correspondingly.

Here, Figure 7 depicted the outcomes of the sensitivity analysis for C-rate of C/10. From Figure 7a we can see, when solid diffusivity values in lithiation were cycle changing, curves pattern were also changing significantly. Same cases were witnessed in delithiation cycle as shown on Figure 7b. Therefore, it can be stated that solid diffusivity has impact on voltage hysteresis. Once best fitted values were found for both the diffusivities, sensitivity analysis was conducted with exchange current density, first we started with lithiation cycle and it was noticed, bottom lines in the curves were fluctuating in vertical y-direction when the values were changing. It shows voltages were changing heavily as shown in Figure 7c. Once the best values for exchange current density in lithiation cycle were found, our focus were moved to delithiation cycle and same techniques were implemented.

As shown in Figure 7d, voltages were changing in vertical y-direction. This time bottom lines were fixed; only upper lines were moving when the values of $i_{0,d}$ changed. It can be seen, from Figure 7c and d, voltage values were changed, when exchange current density values were fluctuated. So, it can be said from the observation that exchange current density is a source of voltage hysteresis. Next, sensitivity analysis with partial molar volume, Ω was conducted. In case of Ω, constant values were used throughout the lithiation-delithiation cycling. Some impacts from Ω were seen, but this parameter is also connected with diffusivity as reported by various researchers at their work (Verbrugge et al., 2015; Verbrugge and Cheng, 2019; Sethuraman et al., 2010; Sethuraman et al., 2012; Hossain et al., 2020b; Hossain, 2021), so again it suggests that solid diffusivity has influence on voltage hysteresis.

Likewise, partial molar volume, for Young's modulus, E and Poisson's ratio, ν, constant values were used for the entire cycling. For both the cases, very little effect from these parameters on voltage hysteresis was observed. The above-mentioned strategies were implemented for

Table 2. List of model parameters used in the study.

Parameter	Value	Units	Reference/remarks
Columbic capacity, $\hat{C}$	Calculated from experiment	mAh/g	Measured; used here
C-Rate, C_{Rate}	Calculated from experiment	1/h	Measured; used here
Deformation-independent surface tension, τ_0	1	J/m^2	Jin et al., 2019; Hossain and Kim, 2020a;
Density of silicon, ρ	2330	kg/m^3	Hossain, 2021; Pal et al., 2014; Hossain and Kim, 2020b;
	8.46×10^{-7}		Sethuraman et al., 2012
Exchange current density, i_0	12.6	A/m^2	Wang et al., 2017
	1.0×10^{-2}		Hossain et al., 2020a; Chandrasekaran et al., 2010
	0.1		Hossain et al., 2020b
Exchange current density for lithiation, i_{0l}	0.006	A/m^2	Measured; used here
Exchange current density for delithiation, i_{0d}	0.008	A/m^2	Measured; used here
Faraday constant, F	96487	C/mol	Hossain, 2021; Pal et al., 2014; Hossain and Kim, 2020a
Initial concentration, c_0	$\times_0 \times \mathrm{c}_{\mathrm{max}\times}$	mol/m^3	Pal et al., 2014; Hossain and Kim, 2020a
Initial particle radius, r_0	2.1×10^{-6}	m	Wang et al., 2013
Initial SOC of silicon 0.000, x_0	0.0001		Pal et al., 2014; Hossain and Kim, 2020b
Mass of the cell, m	1.043798×10^{-3}	kg	Measured
Maximum concentration, c_{max}	$\rho X \frac{Capa}{F}$	mol/m^3	Measured; used here
Partial molar volume, Ω	4.5×10^{-6}	m^3/mol	Pal et al., 2014; used here
	4.625×10^{-6}		Jin et al., 2019
	5.0×10^{-6}		Hossain and Kim, 2020a
	1.0×10^{-5}		Hossain and Kim, 2020b
Poisson's ratio constant, v	0.20		Hossain and Kim, 2020a
	0.28		Pal et al., 2014; used here
	0.27		Jin et al., 2019
	0.45		Hossain and Kim, 2020b
Solid diffusivity, D_s	2.0×10^{-16}	m^2/s	Jin et al., 2019
	3.0×10^{-16}		Wang et al., 2017
	1.0×10^{-17}		Jagannathan and Chandran, 2014
	1.18×10^{-18}		Safari and Delacourt, 2011
Solid diffusivity for lithiation, D_l	2.0×10^{-15}	m^2/s	Measured; used here
Solid diffusivity for delithiation, D_d	5.0×10^{-15}	m^2/s	Measured; used here
Surface modulus, K^s	5	N/m	Hossain, 2021; Pal et al., 2014; Hossain and Kim, 2020b;
Temperature, T	298	K	Hossain, 2021; Pal et al., 2014; Hossain and Kim, 2020b;
Thickness of electrode, L	116×10^{-6}	m	Hossain, 2021; Pal et al., 2014; Hossain and Kim, 2020b

Table 2. Cont'd

Universal gas constant, R_g	8.314	J/mol/K	Hossain, 2021; Hossain et al., 2022a; Hossain et al., 2022b
Volume ratio of silicon, ε	0.6517		Hossain and Kim, 2020a
Young's modulus constant, E	90	GPa	Pal et al., 2014; used here
	100		Jin et al., 2019
	120		Wang et al., 2017
	150		Hossain and Kim, 2020b

Source: Author2022

other C-rates like C/5, C/3 and C/2. In all the cases, large impact from the solid diffusivity and exchange current density on the voltage hysteresis were spotted. Even though initially we used asymmetric values for Ω, E, ν, it did not make any difference in the voltage curve. Therefore, for these three parameters, constant values were chosen throughout the entire cycle. Apart from D_l, D_d, $i_{0,l}$, $i_{0,d}$, Ω, E and ν changing the values of other parameters did not make any difference to voltage curves. Therefore, it can be said solid diffusivity, exchange current density, partial molar volume, Young's modulus and Poisson's ratio are the key parameters which can be used to analyze voltage hysteresis emergence on silicon anode based lithium half cells.

Best fitted result

The best fitted values for the parameters were found after completing sensitivity analysis. Then, all the same parameters were used in our mathematical equations to generate simulation results. Apart from specific capacity of the experimental results, the exact same parameters were used for all for different C-rates. From Figure 8, it can be seen that the simulation results generated by mathematical models were matching with the experimental results. Form the observation, it is to be observed, $D_d = 5.0\times10^{-15}$ (m^2/s) is higher than $D_l = 2.0\times10^{-15}$ (m^2/s).

Li et al. reported it that silicon (Si) goes through compressive stress during lithiation and tensile stress during delithiation (Li et al., 2014). Similarly, it is observed that delithiated exchange current density ($i_{0,d} = 0.008$ A/m^2) is also higher than lithiated exchange current density ($i_{0,l} = 0.006$ A/m^2). We understand that it could be because of solid electrolyte interphase (SEI) layer formation across the silicon (Si) spherical particle during lithiation-delithiation battery cycling.

As stated earlier, Si undergoes volume expansion during lithiation, therefore, more surface crack generation will appear on the surface of the spherical particle, as a result fresh surfaces will be revealed. In consequence, more side reactions will take place because of chemical kinetics. Therefore, more effect from the exchange current densities will be noticed. At the same time, matching of simulation results and experimental results suggested that our mathematical model development is correct.

Influence of stress induced voltage

Here, Butler-Volmer (BV) equation is modified with the addition of hydrostatic stress. By inserting hydrostatic stress term in the Butler-Volmer (BV) equation, maximum of 0.0018 (V) voltage was captured for all four different C-Rates as it showed in Figure 9.

Figure 9 shows stress induced voltage values are significantly low to have solitary impact on voltage hysteresis generation. On the other hand, significantly high influence from asymmetric diffusivity and asymmetric exchange current density on the voltage hysteresis was witnessed. So, it can be said that diffusivity and exchange current density are equally essential for voltage hysteresis occurrence on silicon anode-based lithium half cells.

Conclusion

In this work, the cause of voltage hysteresis occurrence during lithiation-delithiation cycling of Si anode-based lithium half cells by combining experimental and modeling techniques is thoroughly investigated. Voltage hysteresis is identified during lithiation-delithiation battery cycling. A physics-based mathematical model is developed to define the main reason behind voltage hysteresis. Earlier model developers thought that hydrostatic stress generation is the

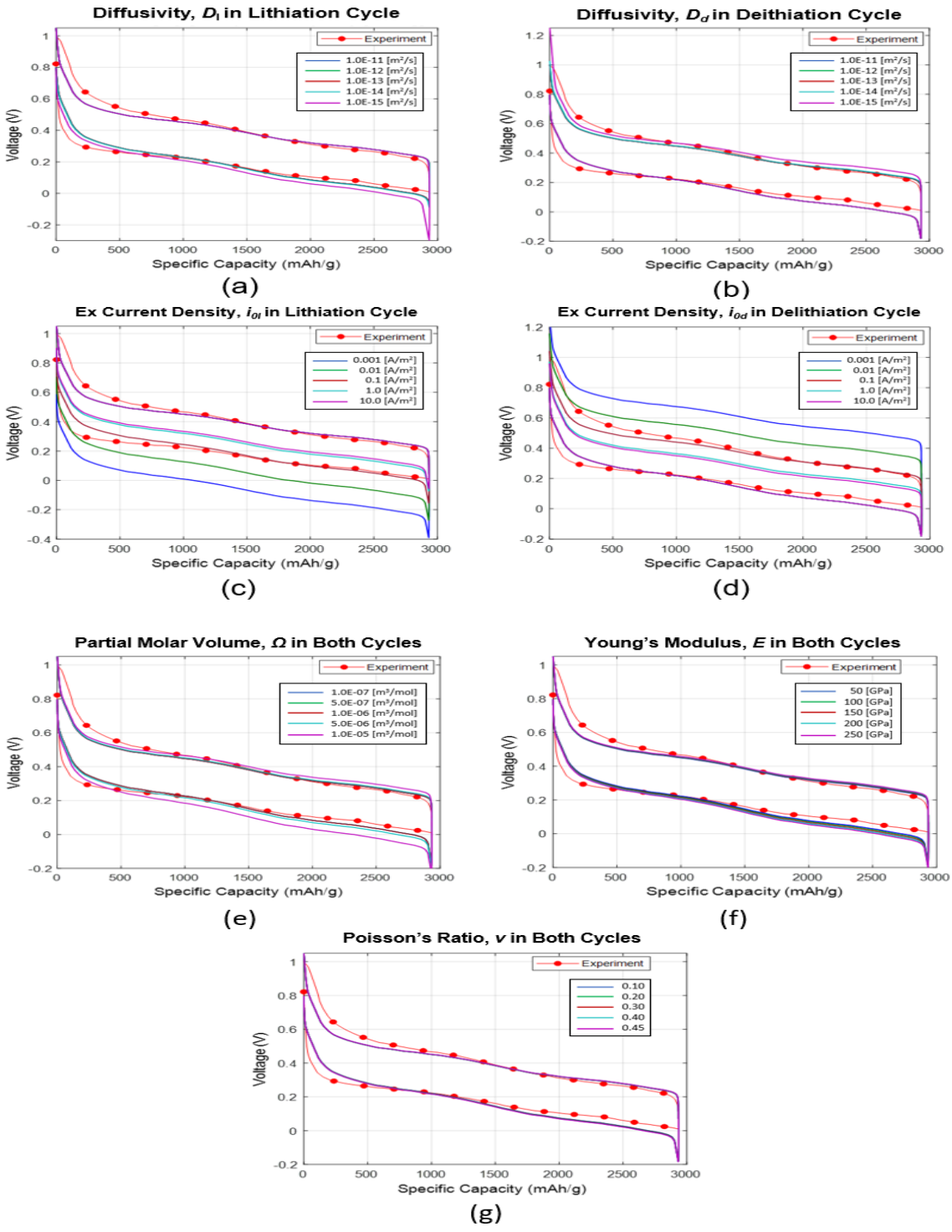

Figure 7. Sensitivity analysis test conducted; (a) Diffusivity in lithiation cycle; (b) Diffusivity in delithiation cycle; (c) Exchange current density in lithiation cycle; (d) Exchange current density in delithiation cycle; (e) Partial molar volume in both cycles; (f) Young's modulus in both cycle; (g) Poisson's ratio in both cycles. Set-1 parametric values are: D_l = 1.0E-11 (m^2/s), D_d = 1.0E-11 (m^2/s), i_{0l} = 0.001 (A/m^2), i_{0d} = 0.001 (A/m^2), Ω = 1.0E-7 (mol/m^3), E = 50 (GPa), v = 0.10; Set-2 values are: D_l = 1.0E-12 (m^2/s), D_d = 1.0E-12 (m^2/s), i_{0l} = 0.01 (A/m^2), i_{0d} = 0.01 (A/m^2), Ω = 5.0E-7 (mol/m^3), E = 100 (GPa), v = 0.20; Set-3 values are: D_l = 1.0E-13 (m^2/s), D_d = 1.0E-13 (m^2/s), i_{0l} = 0.1 (A/m^2), i_{0d} = 0.1 (A/m^2), Ω = 1.0E-6 (mol/m^3), E = 150 (GPa), v = 0.30; Set-4 values are: D_l = 1.0E-14 (m^2/s), D_d = 1.0E-14 (m^2/s), i_{0l} = 1.0 (A/m^2), i_{0d} = 1.0 (A/m^2), Ω = 5.0E-6 (mol/m^3), E = 200 (GPa), v = 0.40; Set-5 values are: D_l = 1.0E-15 (m^2/s), D_d = 1.0E-15 (m^2/s), i_{0l} = 10.0 (A/m^2), i_{0d} = 10.0 (A/m^2), Ω = 1.0E-5 (mol/m^3), E = 250 (GPa), v = 0.45.
Source: Author 2022

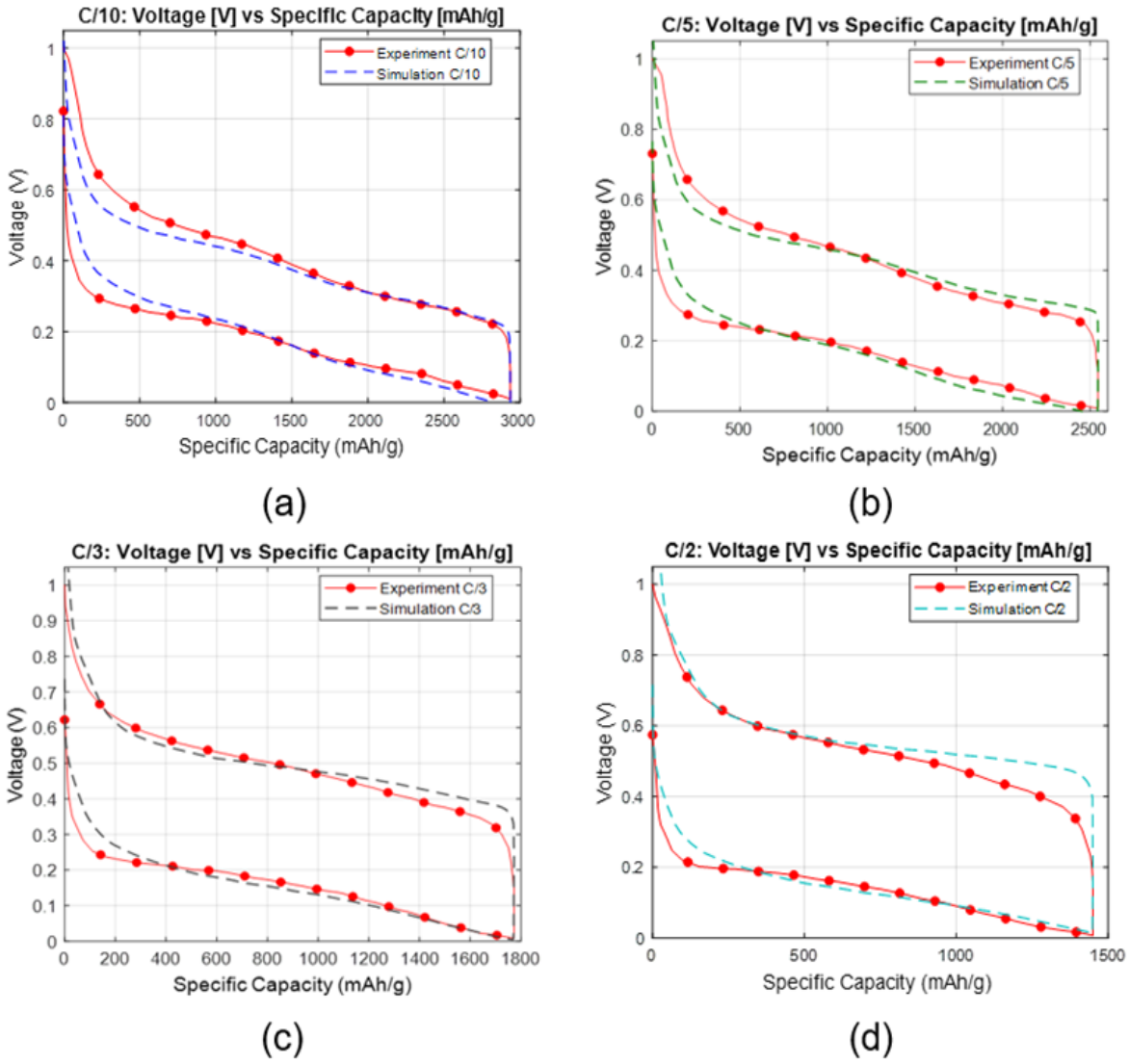

Figure 8. Best fitted validated results of Voltage vs. Specific Capacity graphs at different C-rates: (a) C/10 (b) C/5 (c) C/3 (d) C/2; Exact parameters are used for all different C-rates except specific capacity.
Source: Author 2022

diffusivity is used because of tensile-compressive stress generation during battery cycling. In addition to that, asymmetric exchange current density is implemented because of surface crack generation at the surface of the particle. Most importantly, experimental data is used to validate simulated results generated by mathematical model. Literature surveys were performed to find best fitted parametric values. Key parameters are identified which can control the voltage curves for four different C-rates. It is observed that diffusivity and exchange current density values are higher in delithiation cycle, then lithiation cycle. Stress induced voltage curves are generated as well to check the solitary impact on voltage hysteresis generation. The values are found to have small impact on voltage hysteresis. Whereas, by controlling diffusivity and exchange current density, shape of the curves can be controlled to have a good fit with experimental voltage curves. Therefore, it can be said that not only hydrostatic stress, but also solid diffusivity and exchange current density are equally essential for voltage hysteresis emergence during battery cycling in silicon anode-based lithium half cells.

SYMBOLS

i_{app}, Applied current density (A); c_{av}, average concentration (mol/m^3); L, cell thickness (m); τ_0,

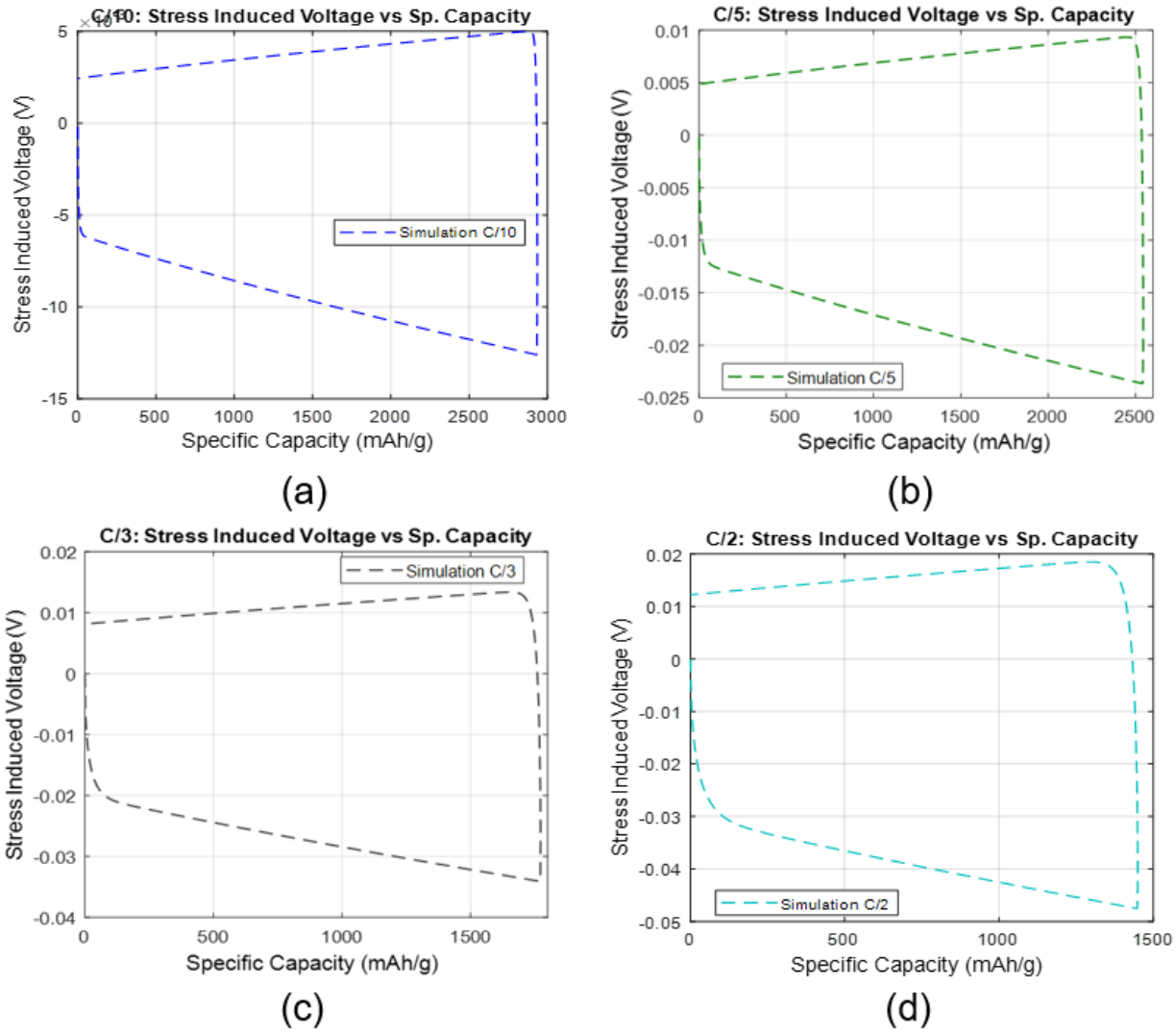

Figure 9. Stress induced voltage vs. specific capacity graphs generated at different C-rates: (a) C/10 (b) C/5 (c) C/3 (d) C/2. Maximum stress induced voltage of 0.40 (V) was to capture by this model.
Source: Author 2022

deformation-independent surface tension (J/m^2); $\boldsymbol{i_{0,d}}$, exchange current density for delithiation (A/m^2); $\boldsymbol{i_{0,l}}$, exchange current density for lithiation (A/m^2); $\boldsymbol{i_{0,SR}}$, exchange current density on side-reaction (A/m^2); $\boldsymbol{F}$, Faraday's constant (C/mol); $\boldsymbol{S_1}$, hydrostatic constant^{-1}; $\boldsymbol{S_2}$, hydrostatic constant^{-2}; $\boldsymbol{\sigma_h}$, hydrostatic stress (MPa); $\boldsymbol{c_0}$, initial lithium concentration (mol/m^3); $\boldsymbol{r_0}$, initial particle radius (m); $\boldsymbol{c_s}$, lithium concentration (mol/m^3); $\boldsymbol{j_n}$, net flux (mol/m^{2}s); $\boldsymbol{N}$, number of particles; $\boldsymbol{U_{Side}}$, open circuit potential on side-reaction (V); $\boldsymbol{\Omega}$, partial molar volume (m^3/mol); $\boldsymbol{R}$ particle radius as function of SOC (m); $\boldsymbol{\nu}$, Poisson's ratio; $\boldsymbol{C_{Rate}}$, rate of charging/discharging; $\boldsymbol{D_d}$, solid diffusivity for delithiation (m^2/s); $\boldsymbol{D_l}$, solid diffusivity for lithiation (m^2/s); $\boldsymbol{SEI}$, solid-electrolyte interphase; $\boldsymbol{SOC}$, state of charge; $\boldsymbol{K^s}$, surface modulus (N/m); $\boldsymbol{a_V}$, surface-to-volume ratio; $\boldsymbol{T}$, temperature (K); $\boldsymbol{\alpha_R}$, transfer co-efficient for the side-reaction; $\boldsymbol{R_g}$, universal gas constant (J/mol/k); $\boldsymbol{V}$, voltage measured during experiment (V); $\boldsymbol{\varepsilon}$, volume ratio of silicon; $\boldsymbol{E}$, Young's modulus (GPa).

CONFLICT OF INTERESTS

The authors have not declared any conflict of interests.

ACKNOWLEDGEMENTS

I'm grateful to the Department of Mechanical Engineering of Washington State University for permitting us to use licensed version of COMSOL Multiphysics, MATLAB and Solid Works. All the encouragement and support I received are outstanding.

REFERENCES

Ashuri M, He Q, Shaw L (2016). Silicon as a potential anode material for Li-ion batteries: where size, geometry and structure matter. Nanoscale 8:74-103.

Baker D, Verbrugge M, Xiao X (2017). An approach to characterize and clarify hysteresis phenomena of lithium-silicon electrodes. Journal of Applied Physics 122:165102.

Boukamp B, Lesh G, Huggins R (1981). All-Solid Lithium Electrodes with Mixed-Conductor Matrix. Journal of the Electrochemical Society 128:725-729.

Bower A, Guduru P, Sethuraman V (2011). A finite strain model of stress, diffusion, plastic flow, and electrochemical reactions in a lithium-ion half-cell. Journal of the Mechanics and Physics of Solids 59:804-828.

Chandrasekaran R, Magasinski A, Yushin G, Fuller T (2010). Analysis of Lithium Insertion/Deinsertion in a Silicon Electrode Particle at Room Temperature. Journal of the Electrochemical Society 157:A1139-A1151.

Cheng Y, Verbrugge M (2018). The influence of surface mechanics on diffusion induced stresses within spherical nanoparticles. Journal of Applied Physics 104:083521.

Christensen J, Newman J (2006). A Mathematical Model of Stress Generation and Fracture in Lithium Manganese Oxide. Journal of the Electrochemical Society 153:A1019.

Di Leo C, Rejovitzky E, Anand (2015). Diffusion–deformation theory for amorphous silicon anodes: The role of plastic deformation on electrochemical performance. International Journal of Solids and Structures 67-68:283-296.

Hossain A (2021). Development of a mathematical model to study the impact of state of charge dependent exchange current density on the generated voltage hysteresis of silicon anode-based lithium half cells. Journal of Mechanical Engineering Research 12(1):37-48.

Hossain A, Cha Y, Song M, Kim S (2020a). Side Reaction Correction and Non-linear Exchange Current Density for Mathematical Modeling of Silicon Anode Based Lithium-Ion Batteries. Available at: https://www.vancouver.wsu.edu/research-showcase/researchshowcase-gallery-poster-2207 (Accessed on November 15, 2022).

Hossain A, Masud N, Yasin M, Ali M (2020b). Analysis of the Performance of Microbial Fuel Cell as a Potential Energy Storage Device". Proceedings of International Exchange and Innovation Conference on Engineering & Sciences (IEICES) 6:149-155

Hossain A, Kim S (2020a). Development of a physics-based mathematical model to analyze the limitations of microparticle silicon-based lithium half cells IMECE Technical Presentation. Available at: https://www.researchgate.net/publication/346031457_Development_of_a_PhysicsBased_Mathematical_Model_to_Analyze_the_Limitations_of_Microparticle_Silicon_Based_Lithium_Half_Cells_IMECE_Technical_Presentation (Accessed on November 15, 2022).

Hossain A, Kim S (2020b). Washington State University, degree granting institution. Development of a Physics-Based Mathematical Model of Microparticle Silicon Based Lithium Half Cells. Available at: http://www.dissertations.wsu.edu/Thesis/Fall2020/A_Hossain_121420.pdf (Accessed on November 12:2022.

Hossain A, Masud N, Ali M (2022a). Comprehensive cost analysis of electrochemical performance in microbial fuel cells. Microbial Fuel Cells: Emerging Trends in Electrochemical Applications. IOP Publications 350(1):13.

Hossain A, Masud N, Roy S, Ali M (2022b). Investigation of voltage storage capacity for the variation of electrode materials in microbial fuel cells with experimentation and mathematical modelling. International Journal of Water Resources and Environmental Engineering. 14(4):97-109.

Jagannathan M, Chandran K (2014). Analytical modeling and simulation of electrochemical charge/discharge behavior of Si thin film negative electrodes in Li-ion cells. Journal of Power Sources 247:667-675.

Jin C, Li H, Song Y, Lu B, Soh A, Zhang J (2019). On stress-induced voltage hysteresis in lithium ion batteries: Impacts of surface effects and inter-particle compression. Science China Technological Sciences 62:1357-1364.

Jin Y, Zhu B, Lu Z, Liu N, Zhu J (2017). Challenges and Recent Progress in the Development of Si Anodes for Lithium-Ion Battery. Advanced Energy Materials 7:1700715.

Li J, Dudney N, Xiao X, Cheng Y, Liang C, Verbrugge M (2014). Asymmetric Rate Behavior of Si Anodes for Lithium-Ion Batteries: Ultrafast Delithiation versus Sluggish Lithiation at High Current Densities. Advanced Energy Materials 5:1401627.

Liang B, Liu Y, Xu Y (2014). Silicon-based materials as high capacity anodes for next generation lithium ion batteries. Journal of Power Sources 267:469-490.

Lu B, Song Y, Zhang Q, Pan J, Cheng Y, Zhang J (2016). Voltage hysteresis of lithium ion batteries caused by mechanical stress. Physical Chemistry Chemical Physics 18:4721-4727.

Masud N, Hossain A, Moresalein M, Ali M (2021). Performance Evaluation of Microbial Fuel Cell with Food Waste Solution as a Potential Energy Storage Medium. Proceedings of International Exchange and Innovation Conference on Engineering and Sciences 7:96-102.

Ojeda B, Waliullah M, Hossain A, Nguyen T, Wettstein T, Tadesse Y, Bernal R (2022). High-throughput tensile testing of silver nanowires. Extreme Mechanics Letters 101896.

Pal S, Damle S, Patel S, Datta M, Kumta P, Maiti S (2014). Modeling the delamination of amorphous-silicon thin film anode for lithium-ion battery. Journal of Power Sources 246:149-159.

Pharr M, Suo Z, Vlassak J (2013). Measurements of the fracture energy of lithiated silicon electrodes of li-ion batteries. Nano Letters 13:5570-5577.

Safari M, Delacourt C (2011). Mathematical Modeling of Lithium Iron Phosphate Electrode: Galvanostatic charge/discharge and path dependence. Journal of the Electrochemical Society 158(2):A63-A73.

Sethuraman V, Srinivasan V, Bower A, Guduru P (2010). In Situ Measurements of Stress-Potential Coupling in Lithiated Silicon. Journal of The Electrochemical Society 157:A1253.

Sethuraman V, Srinivasan V, Newman J (2012). Analysis of Electrochemical Lithiation and Delithiation Kinetics in Silicon. Journal of The Electrochemical Society 160:A394-A403.

Sikha G, De S, Gordon J (2014). Mathematical model for silicon electrode – Part I. 2-d model. Journal of Power Sources 262:514-523.

Song Y, Soh A, Zhang J (2016). On stress-induced voltage hysteresis in lithium ion batteries: impacts of material property, charge rate and particle size. Journal of Materials Science, pp. 9902-9911.

Tanim T, Rahn C, Wang C (2015). State of charge estimation of a lithium-ion cell based on a temperature dependent and electrolyte enhanced single particle model. Energy 80:731-739.

Tarascon J, Armand M (2001). Issues and challenges facing rechargeable lithium batteries. Nature 414:359-367.

Verbrugge M, Baker D, Xiao X, Zhang Q, Cheng Y (2015). Experimental and Theoretical Characterization of Electrode Materials that Undergo Large Volume Changes and Application to the Lithium–Silicon System. The Journal of Physical Chemistry C 119:5341-5349.

Verbrugge M, Cheng Y (2019). Stress Distribution within Spherical Particles Undergoing Electrochemical Insertion and Extraction. ECS Transactions 16:127-139.

Wang C, Wu H, Chen Z, McDowell M, Cui Y, Bao Z (2013). Self-healing chemistry enables the stable operation of silicon microparticle anodes for high-energy lithium-ion batteries. Nature Chemistry 5:1042-1048.

Wang M, Xiao X, Huang X (2017). A multiphysics microstructure-resolved model for silicon anode lithium-ion batteries. Journal of Power Sources 348:66-79.

Wu H, Cui Y (2012). Designing nanostructured Si anodes for high energy lithium ion batteries. Nano Today 7:414-429.

Zhang W (2010). A review of the electrochemical performance of alloy anodes for lithium-ion batteries. Journal of Power Sources 196:13-24.

Zhang X, Shyy W, Marie Sastry A (2007). Numerical Simulation of Intercalation-Induced Stress in Li-Ion Battery Electrode Particles. Journal of The Electrochemical Society 154:A910.

APPENDIX

Modification of Butler-Volmer (BV) Equation: For battery modeling, Butler-Volmer (BV) Equation is one of the most essential parts. Here we included the modified version of BV equation (3) where stress induced voltage part is included.

$$\frac{i_{app}}{a_V LF} = \frac{i_0}{F}\left\{\exp\left[(1-\alpha)\frac{F(V-U)-\sigma_h\Omega}{R_g T}\right] - \exp\left[-\alpha\frac{F(V-U)-\sigma_h\Omega}{R_g T}\right]\right\} \quad \text{(A1)}$$

Here, $\sigma_h\Omega$ is called the stress induced voltage. Cheng and Verbrugge (2018), Jin et al. (2019) and Hossain (2021) and Zhang et al. (2007) all indicated how important it is to include this additional term in BV equation. i_0 is called the exchange current density. The following equation is generally used to calculate this value:

$$i_0 = F k_0 c_L^{1-\alpha}(c_{\max} - c_{\text{surf}})^{1-\alpha} c_{\text{surf}}^{\alpha} \quad \text{(A2)}$$

Where k_0 is known as Rate constant and $c_{\text{surf}\ \&}\ c_L$ are known as surface concentration (mol/m^3) and concentration of electrolyte (mol/m^3). But, in our model, we used asymmetric exchange current density values instead of going with Equation (*A2*).

Butler-Volmer equation can be derived as follow, for lithium insertion into the silicon:

$$LiSi \rightarrow Li^+ + e^- + Si \quad \text{(A3)}$$

The OCP, U can be expressed as:

$$FU = \mu_{Li}^0 + \mu_{si} - \mu_{LiSi} \quad \text{(A4)}$$

The electrochemical potential μ_{LiSi} can be expressed with the mechanical stress as:

$$\mu_{LiSi} = \mu_{LiSi}^0 + R_g T \ln ax + \Omega\sigma_h \quad (A5)$$

Where μ_0a constant value at reference state is, R_g is the gas constant, T is the temperature, a is the activity coefficient, x is the mole fraction, and σ_h is hydrostatic stress. So,

$$FU = \mu_{Li}^0 + \mu_{si} - \mu_{LiSi}^0 - R_g T \ln ax - \Omega\sigma_h \quad \text{(A6)}$$

Therefore, we may have shift in the OCP by the mechanical stress, and the OCP with mechanical stress, U_{st}

$$U_{st} = U + \frac{\Omega\sigma_h}{F} \quad \text{(A7)}$$

Then, in the cell-level modeling, this can be included in the Butler-Volmer equation:

$$j_n = \frac{i_0}{F}\left\{\exp\left[(1-\alpha)\frac{F(V-U)-\sigma_h\Omega}{R_g \mathrm{T}}\right] - \exp\left[-\alpha\frac{F(V-U)-\sigma_h\Omega}{R_g \mathrm{T}}\right]\right\} \quad (A8)$$

If the symmetric coefficient $\alpha = 1/2$

$$\frac{j_n F}{2i_0} = \sinh\frac{F(V-U)-\sigma_h\Omega}{2R_g \mathrm{T}} \quad \text{(A9)}$$

Or

$$V = U + \frac{\sigma_h\Omega}{\mathrm{F}} + \frac{2R_g T}{F}\operatorname{asinh}\frac{j_n F}{2i_0} \quad \text{(A10)}$$

Putting the value of flux value j_n the above equation can be written as,

$$V = U + \frac{\sigma_h\Omega}{\mathrm{F}} + \frac{2R_g T}{F}\sinh^{-1}\left(\frac{i_{app}}{2i_0 a_V\, LF}\right) \quad \text{(A11)}$$

Here, V is the Voltage (V) and other parameters have been discussed. We used this Equation (Cheng and Verbrugge, 2018) in our model to generate several results.

Development of radius equation as a function of SOC: This is the most important feature of our model. As it was mentioned earlier silicon particle experiences ~300% expansion during lithiation and contraction during delithiation. Therefore, the radius of the particle also experiences a change of radius as the state of charge (SOC) progresses. Derivation of particle radius has been discussed here. When the particle is fully delithiated, the SOC is 0, we considered the particle volume as $V = V_0$. Since, silicon experiences ~300% volume expansion during lithiation. At fully lithiatied condition, when SOC=1, Final particle volume becomes as $V = 3V_0$.

Since, we are considering spherical particle. Therefore, we considered volume equation as $V = \frac{4}{3}\pi r^3$. Following schematic diagram shows the working principle:

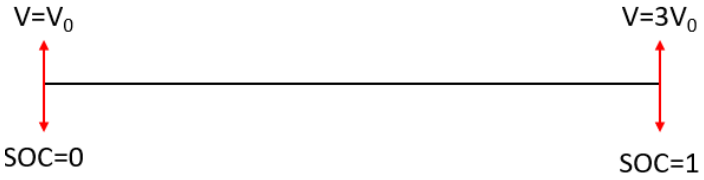

Here, When SOC = 0, $V_i = V_0$ and at SOC =1, $V_f = 3V_0$. The volume equation is developed as shown:

$$V(SOC) = V_0 + SOC(V_f - V_i)$$
$$\Rightarrow V(SOC) = V_0 + SOC(3V_0 - V_0) \quad \text{(At fully lithiated state)}$$
$$\Rightarrow V(SOC) = V_0 + SOC(2V_0)$$
$$\Rightarrow V(SOC) = V_0(1 + 2SOC)$$
$$\Rightarrow \frac{4}{3}\pi r^3(SOC) = \frac{4}{3}\pi r_0^3(1 + 2SOC)$$
$$r(SOC) = r_0\sqrt[3]{(1 + 2SOC)}$$

Therefore, our own developed equation can be written as follows:

$$R = r_0[1 + (2SOC)]^{\frac{1}{3}} \qquad \text{(A12)}$$

Here, r_0 is defined as initial particle radius. SOC is regarded as the State of Charge. $r_0(SOC)$ is defined as the particle radius equation as a function of SOC. $r_0(SOC)$ can be denoted as R. We are the first one to include this feature in mathematical battery model development.